Neural network study of hidden-charm pentaquark resonances

Halil Mutuk[1)]

Physics Department, Faculty of Arts and Sciences, Ondokuz Mayis University, Samsun 55139, Turkey

Abstract: Recently, the LHCb experiment announced the observation of hidden-charm pentaquark states $P_c(4312)$, $P_c(4440)$, and $P_c(4457)$ near $\Sigma_c\bar{D}$ and $\Sigma_c\bar{D}^*$ thresholds. In this present work, we studied these pentaquarks in the framework of the nonrelativistic quark model with four types of potential. We solved five-body Schrödinger equation by using the artificial neural network method and made predictions of parities for these states, which are not yet determined by experiment. The mass of another possible pentaquark state near the $\bar{D}^*\Sigma_c^*$ with $J^P = 5/2^-$ is also calculated.

Keywords: hidden-charm resonances, pentaquark, neural networks

1   Introduction

In recent years, some experimental states or resonances have been announced as observable candidates beyond the conventional quark-antiquark and three-quark configurations. Most of these particles are not confirmed with high statistics and better resolution. Moreover, except for the case for $X(3872)$ [1], they were observed only in a single experiment, such as $X(5568)$ [2, 3] or in one type of experiment, such as B factories. The observation of $X(3872)$ was a milestone for the era of so-called exotic states. Exotic states are beyond the description of the conventional quark model. The pentaquark represents an example of these exotic states. It consists of four quarks ($qqqq$) and one antiquark ($\bar{q}$) bound together.

This situation turned into a new perspective with the first discovery of the pentaquark candidates, $P_c(4450)$ and $P_c(4380)$ by LHCb in 2015 [4]. Theoretical studies were perfomed for these pentaquark particles prior to their observation [5–8]. The masses of these states were very close to $\bar{D}^*\Sigma_c^*$ threshold. This justifies the assumption that those two pentaquarks as baryon-meson molecule [9–19]. The other possibilities are the compact pentaquark [20–23], quark model [24–26], chiral quark model [27], quark-cluster model [28] and baryocharmonium model [29].

Most recently, the LHCb collaboration updated the results of Ref. [4] reporting the observation of new nar-

row pentaquark states [30] with masses and widths as follows:

$$P_c(4312)\ M = (4311.9 \pm 0.7^{+6.8}_{-0.6})\ \text{MeV},$$
$$\Gamma = (9.8 \pm 2.7^{+3.7}_{-4.5})\ \text{MeV},$$
$$P_c(4440)\ M = (4440.3 \pm 1.3^{+4.1}_{-4.7})\ \text{MeV},$$
$$\Gamma = (20.6 \pm 4.9^{+8.7}_{-10.1})\ \text{MeV},$$
$$P_c(4457)\ M = (4457.3 \pm 0.6^{+4.1}_{-1.7})\ \text{MeV},$$
$$\Gamma = (6.4 \pm 2.0^{+5.7}_{-1.9})\ \text{MeV}.$$

The masses of $P_c(4440)$ and $P_c(4457)$ are close to $\Sigma_c\bar{D}^*$ threshold, and the mass of $P_c(4312)$ is very close to $\Sigma_c\bar{D}$ threshold. As pointed out in [31], the central mass of the $P_c(4312)$ state is ~6 MeV below the $\Sigma_c^+\bar{D}^0$ threshold and ~12 MeV below the $\Sigma_c^{++}D^-$ threshold. For $P_c(4440)$, it is ~20 MeV below the $\Sigma_c^+\bar{D}^{*0}$ and ~24 MeV below the $\Sigma_c^{++}\bar{D}^{*-}$ thresholds. In the case of $P_c(4457)$, it is ~3 MeV below the $\Sigma_c^+\bar{D}^{*0}$ and ~7 MeV below the $\Sigma_c^{++}\bar{D}^{*-}$ thresholds. The isospin violating process can occur when the width of a resonance is small and mass is below the corresponding thresholds. This can be an example for these pentaquarks.

The observation of these pentaquarks received immediate attention [32–39]. In this study, we use the constituent quark model to obtain spectrum and quantum numbers. As mentioned in Ref. [25], the constituent quark model has often been employed for exploratory studies in

QCD and paved the way for lattice simulations and QCD sum rules calculations. The main part of the constituent quark model is to obtain a solution of the Schrödinger equation with a specific potential. For mesons and baryons, this can be done effectively, and one can obtain reliable results comparing to the results of experiments. However, pentaquark structures are multiquark systems and due to the complex interactions among quarks, solving the five-body Schrödinger equation is a challenging task. For this purpose, we solved the Schrödinger equation via an artificial neural network (ANN).

Apart from their application in other fields, ANNs can be utilized as an elective strategy to solve differential conditions and quantum mechanical systems [40, 41]. ANNs provide some advantages compared to standard numerical methods [42, 43]

● The solution is continuous over the entire domain of integration,

● With the number of sampling points and dimensions of the problem, the computational complexity does not increase significantly,

● Rounding-off error propagation of standard numerical methods does not influence the neural network solution,

● The method requires a lower number of model parameters and therefore does not require large memory space in computer.

This paper is organized as follows. In Section 2, the model and method used for the calculations are described. In Section 3, obtained results are discussed, and in Section 4, we sum up our work.

2 Model and method

2.1 Model

The Hamiltonian of Ref. [44] reads as follows

$$H = \sum_i \left(m_i + \frac{p_i^2}{2m_i} \right) - \frac{3}{16} \sum_{i<j} \tilde{\lambda}_i \tilde{\lambda}_j v_{ij}(r_{ij}) \tag{1}$$

with the potential

$$v_{ij}(r) = -\frac{\kappa(1 - e^{-\frac{r}{r_c}})}{r} + \lambda r^p + \Lambda +$$

$$\frac{2\pi}{3 m_i m_j} \kappa'(1 - e^{-\frac{r}{r_c}}) \frac{e^{-\frac{r^2}{r_0^2}}}{\pi^{3/2} r_0^3} \sigma_{\mathbf{i}} \sigma_{\mathbf{j}}, \tag{2}$$

where $r_0(m_i, m_j) = A\left(\frac{2m_i m_j}{m_i + m_j}\right)^{-B}$, A and B are constant parameters, κ and κ' are parameters, r_{ij} is the interquark distance $|\mathbf{r_i} - \mathbf{r_j}|$, σ_i are the Pauli matrices and $\tilde{\lambda}_i$ are Gell-Mann matrices. There are four potentials referred to the p nd r_c:

$$AL1 \rightarrow p = 1, \ r_c = 0,$$
$$AP1 \rightarrow p = 2/3, \ r_c = 0,$$
$$AL2 \rightarrow p = 1, \ r_c \neq 0,$$
$$AP2 \rightarrow p = 2/3, \ r_c \neq 0.$$

The related parameters are given in Table 1.

This potential was developed under the nonrelativistic quark model (NRQM) and used for exploratory studies. It is composed of a 'Coulomb + linear' or 'Coulomb + 2/3-power' term and a strong but smooth hyperfine term. Further details on this potential are provided in Ref. [44]. They built a new interquark potential, which works equally well on the meson and baryon sector. This simple quark model is based on nonrelativistic kinetic energy and a color-additive interaction related to pairwise forces carried by color-octet exchanges [25].

2.2 Method

Nowadays, machine learning is one of the most popular research fields of modern science. The fundamental ingredient of machine learning systems is artificial neural networks (ANNs), since the most effective way of

Table 1.   Parameters of the potentials.

	AL1	AP1	AL2	AP2
$m_u = m_d$	0.315 GeV	0.277 GeV	0.320 GeV	0.280 GeV
m_s	0.577 GeV	0.553 GeV	0.587 GeV	0.569 GeV
m_c	1.836 GeV	1.819 GeV	1.851 GeV	1.840 GeV
m_b	5.227 GeV	5.206 GeV	5.231 GeV	5.213 GeV
κ	0.5069	0.4242	0.5871	0.5743
κ'	1.8609	1.8025	1.8475	1.8993
λ	0.1653 GeV^2	0.3898 GeV$^{5/3}$	0.1673 GeV^2	0.3978 GeV$^{5/3}$
Λ	−0.8321 GeV	−1.1313 GeV	−0.8182 GeV	−1.1146 GeV
B	0.2204	0.3263	0.2132	0.3478
A	1.6553 GeV^{B-1}	1.5296 GeV^{B-1}	1.6560 GeV^{B-1}	1.5321 GeV^{B-1}
r_c	0	0	0.1844 GeV^{-1}	0.3466 GeV^{-1}

learning is done by ANNs. ANN is a computational model motivated by the biological nervous system. ANN is made up of computing units, called neurons. A schematic diagram of an ANN is given in Fig. 1.
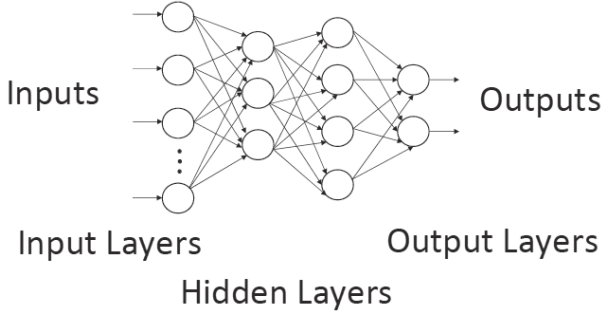

Fig. 1.   A model of multilayer neural networks

In this work, we use a multilayer perceptron (neuron) neural network (MLPN). A MLPN contains more than one layer of artificial neurons. These layers are connected to the next layer, however there is no connection among the neurons in the same layer. They are ideal tools for solving differential equations [45]. A simple model of a neuron can be seen Fig. 2.
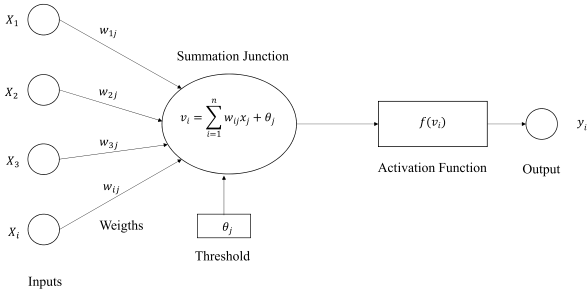

Fig. 2.   A model of single neuron

Feed-forward neural networks, which are used in this present study, are the most used architectures because of their structural flexibility, good representational capabilities, and a wide range of training algorithms available [45]. All input signals are summed together as z, and the nonlinear activation function determines the output signal $\sigma(z)$. We use a sigmoid function

$$\sigma(z) = \frac{1}{1 + e^{-z}} \qquad (3)$$

as an activation function, since all derivatives of $\sigma(z)$ can be derived in terms of themselves. The information process can only flow one-way in feed-forward neural networks, namely from input layer(s) to output layer(s). The input-output properties of the neurons can be written as

$$o_i = \sigma(n_i), \qquad (4)$$

$$o_j = \sigma(n_j), \qquad (5)$$

$$o_k = \sigma(n_k), \qquad (6)$$

where i, j, and k depict the input, hidden, and output layers, respectively. Input to the perceptrons are given as

$$n_i = (\text{Input signal to the neural network}), \qquad (7)$$

$$n_j = \sum_{i=1}^{N_i} \omega_{ij} o_i + \theta_j, \qquad (8)$$

$$n_k = \sum_{i=1}^{N_j} \omega_{jk} o_j + \theta_k, \qquad (9)$$

where N_i and N_j represent the numbers of the units, which belong to input and hidden layers, respectively, ω_{ij} is the synaptic weight parameter connecting the neurons i and j, and θ_j is threshold parameter for the neuron j [46]. The overall response of the network can be written as

$$o_k = \sum_{j=1}^{b_n} \omega_{jk} \sigma \left(\sum_{i=1}^{a_n} \omega_{ij} o_i + \theta_j \right) + \theta_k. \qquad (10)$$

One can obtain the derivatives of o_k with respect to the network parameters (weights and thresholds) by differentiating Eq. (10) as

$$\frac{\partial o_k}{\partial \omega_{ij}} = \omega_{jk} \sigma^{(1)}(n_j) n_i, \qquad (11)$$

$$\frac{\partial o_k}{\partial \omega_{jk}} = \sigma(n_j) \delta_{kk'}, \qquad (12)$$

$$\frac{\partial o_k}{\partial \theta_j} = \omega_{jk} \sigma^{(1)}(n_j), \qquad (13)$$

$$\frac{\partial o_k}{\partial \theta_{k'}} = \delta_{kk'}. \qquad (14)$$

To obtain the spectra of pentaquark states, we consider the ANN application to a quantum mechanical system. We will follow the formalism that was formulated in [40]. Consider the following differential equation

$$H\Psi(r) = f(r) \qquad (15)$$

where H is a linear operator, $f(r)$ is a function and $\Psi(r) = 0$ at the boundaries. To solve this differential equation, it is possible to write a trial function as

$$\Psi_t(\mathbf{r}) = A(\mathbf{r}) + B(\mathbf{r}, \lambda) N(\mathbf{r}, \mathbf{p}), \qquad (16)$$

which feeds a neural network with vector parameter $\mathbf{p}$ and λ to be adjusted later. The parameter $\mathbf{p}$ stands for the weights and biases of the neural network. $A(\mathbf{r})$ and $B(\mathbf{r}, \lambda)$ should be conveniently specified for $\Psi_t(\mathbf{r})$ to satisfy the boundary conditions regardless of the $\mathbf{p}$ and λ values. To solve Eq. (15), the collocation strategy can be utilized, and it can be changed into a minimization problem as

$$\min_{p, \lambda} \sum_i [H\Psi_t(r_i) - f(r_i)]^2. \qquad (17)$$

Eq. (15) can be written as

$$H\Psi(r) = \epsilon \Psi(r) \qquad (18)$$

with the boundary condition $\Psi(r) = 0$. The trial solution can be written of the form

$$\Psi_t(r) = B(\boldsymbol{r}, \lambda) N(\boldsymbol{r}, \boldsymbol{p}), \qquad (19)$$

where $B(\boldsymbol{r}, \lambda) = 0$ at boundary conditions for a variety of λ values. By discretizing the domain of the problem, Eq. (17) can be transformed into a minimization problem with respect to the parameters $\boldsymbol{p}$ and λ

$$E(\boldsymbol{p}, \lambda) = \frac{\sum_i [H\Psi_t(r_i, \boldsymbol{p}, \lambda) - \epsilon\Psi_t(r_i, \boldsymbol{p}, \lambda)]^2}{\int |\Psi_t|^2 \mathrm{d}\boldsymbol{r}}, \qquad (20)$$

where E is the error function, and ϵ can be computed by

$$\epsilon = \frac{\int \Psi_t^* H\Psi_t \mathrm{d}\boldsymbol{r}}{\int |\Psi_t|^2 \mathrm{d}\boldsymbol{r}}. \qquad (21)$$

Considering a multilayer neural network with n input units, one hidden layer with n units and one output, then, for a given input vector

$$\boldsymbol{r} = (r_1, \cdots, r_n), \qquad (22)$$

the output of the network is

$$N = \sum_{i=1}^m v_i \sigma(z_i), \qquad (23)$$

where

$$z_i = \sum_{j=1}^n \omega_{ij} r_j + u_i. \qquad (24)$$

Here, ω_{ij} is the weight from input unit j to hidden unit i, v_i is the weight from hidden unit i to output, u_i is the bias of hidden unit i and $\sigma(z)$ is the sigmoid function, Eq. (3). The derivatives of output can be written as

$$\frac{\partial^k N}{\partial r_j^k} = \sum_{i=1}^m v_i \omega_{ij}^k \sigma_i^{(k)}, \qquad (25)$$

where $\sigma_i = \sigma(z_i)$ and $\sigma^{(k)}$ is the k-th order derivative of the sigmoid.

To obtain desired results, the ANN has to first perform learning. The learning mechanism is the most important property of the ANN. In this work, we used a feed-forward neural network with a back propagation algorithm, which is also known as delta learning rule. This learning rule is valid for the continuous activation function, such as Eq. (3). The algorithm is as follows [47]:

Step 1 Initialize the weights w from the input layer to the hidden layer and weights v from the hidden layer to the output layer. The learning parameter (that lies between 0 and 1) and error $E_{\max}$ are chosen. Initially, the error is assumed to be zero.

Step 2 Train the network.

Step 3 Compute the error value.

Step 4 Compute the error signal terms of the output layer and the hidden layer.

Step 5 Compute components of error gradient vectors.

Step 6 Check the weights if they are properly modified.

Step 7 If $E = E_{\max}$ terminate the training session. If not, go to step 2 with $E \to 0$ and initiate a new training.

We parametrize trial function as

$$\phi_t(r) = re^{-\beta r^2} N(r, \boldsymbol{u}, \boldsymbol{w}, \boldsymbol{v}), \ \beta > 0 \qquad (26)$$

where N denotes the feed forward artificial neural network with one hidden layer and m sigmoid hidden units with

$$N(r, \boldsymbol{u}, \boldsymbol{w}, \boldsymbol{v}) = \sum_{j=1}^m v_j \sigma(\omega_j r + u_j). \qquad (27)$$

The minimization problem becomes as

$$\frac{\sum_i [H\phi_t(r_i) - \epsilon\phi_t(r_i)]^2}{\int |\phi_t(r)|^2 \mathrm{d}r}. \qquad (28)$$

We solved the Schrödinger equation in the interval $0 < r < 1$ fm using 250 equidistant points with $m = 10$. The wave function Eq. (26) can accommodate the observed meson and baryon spectra. It is apparent that the wave functions for mesons and baryons are different from the pentaquarks. In the case of pentaquark states, the wave function contains not only the spatial part, but also spin, color and isospin parts. To solve the five-body problem, Jacobi coordinates can be used [25]:

$$\vec{x} = \vec{r}_2 - \vec{r}_1, \ \vec{y} = \vec{r}_4 - \vec{r}_3, \ \vec{t} = \vec{r}_5 - \frac{\vec{r}_3 + \vec{r}_4}{2}, \qquad (29)$$

$$\vec{z} = \frac{\sum_{i=1}^2 m_i \vec{r}_i}{\sum_{i=1}^2 m_i} - \frac{\sum_{i=3}^5 m_i \vec{r}_i}{\sum_{i=3}^5 m_i}, \ \vec{R} = \frac{\sum_{i=1}^5 m_i \vec{r}_i}{\sum_{i=1}^5 m_i}. \qquad (30)$$

Quark arrangements with these coordinates are shown in Fig. 3.
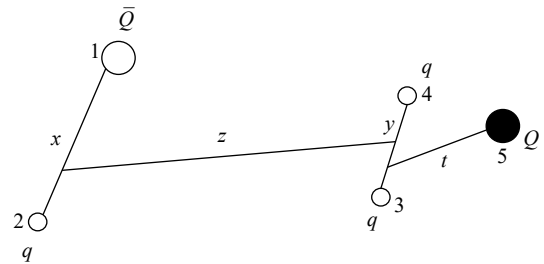
Fig. 3.   Quark configuration with Jacobi coordinates [25]

In this studfy, we use the wave function of Ref. [25], which reads as

$$\Psi = \sum_\alpha \psi_\alpha(\vec{x}, \vec{y}, \vec{z}, \vec{t}) |\alpha\rangle, \qquad (31)$$

$$\psi_\alpha(\vec{x}, \vec{y}, \vec{z}, \vec{t}) = \sum_i \gamma_{\alpha,i} \exp\left(-\tilde{X}^\dagger \cdot A_{\alpha,i} \cdot X/2\right), \qquad (32)$$

where $|\alpha\rangle$ is color spin state, $A_{\alpha,i}$ are 4×4 positive defin-

ite matrices whose elements are the range parameters, and $\tilde{X}^\dagger = \left\{ \vec{x}, \vec{y}, \vec{z}, \vec{t} \right\}$. Color states are calculated with the $SU(3)$ Clebsch-Gordan coefficients using the algorithm given in [48]. Taking into account of spin, there are five independent spin arrangements for $S = 1/2$ resulting 15 color-spin states $|\alpha\rangle$, 4 spin states for $S = 3/2$ resulting 12 color-spin states, 1 spin state for $S = 5/2$ resulting 3 color-spin sates. For the isospin, there are two linearly independent isospin $1/2$ vectors and one isospin $3/2$ vector. Further discussion on color, spin, and isospin is given in Ref. [26]. The range parameters of $A_{\alpha,i}$ in the wave function can be used to minimize the energy. For this purpose, we parametrize Eq. (32) as

$$\phi_t(x_i) = \sum_i \gamma_{\alpha,i} \exp\left(-\tilde{X}^\dagger \cdot A_{\alpha,i} \cdot X/2\right) |\alpha\rangle N(x_i, \boldsymbol{u}, \boldsymbol{w}, \boldsymbol{v}), \quad (33)$$

and the minimization problem becomes

$$\frac{\sum_i \left[H\phi_t(x_i) - \epsilon\phi_t(x_i) \right]^2}{\int |\phi_t(x_i)|^2 \mathrm{d}x_i}. \quad (34)$$

Before solving the five-body Schrödinger equation, some remarks should be made. At first, the quark configuration in Fig. 3 represents asymptotic thresholds. In this configuration, the pentaquark state is composed of an anti-charmed meson and a charmed baryon. Asymptotic thresholds depict possible nominal reachable values, summing the contribution of all quarks. They are reached when the range parameters of the trial function with the Jacobi coordinate of $\vec{z}$ vanish.

The second point is that the mass spectrum depends on the choice of the Hamiltoniand and the trial function. In Ref. [26], the authors used a very similar Hamiltonian

$$H = \sum_i \left(m_i + \frac{\boldsymbol{p}_i^2}{2m_i} \right) - \frac{3}{16} \sum_{i<j} \tilde{\lambda}_i \tilde{\lambda}_j V_{ij}(r_{ij}) \quad (35)$$

where T_G is the kinetic energy of the center-of-mass system and $V_{ij}(r_{ij})$ potentials of [44], and with a different wave function. They calculated threshold energies with this Hamiltonian. To test the choice of the Hamiltonian, they also used the AL1 potential of [44] and found that the results of five-body calculations are essentially not modified.

Based on these arguments, we solved the Schrödinger equation in the interval $0 < x_i < 1$ fm using 250 equidistant points with $m = 10$.

3　Results and discussion

At the first step, we calculated the masses of heavy mesons and baryons with all potentials with the wave function given in Eq. (26). The results are given in Table 2.

Interestingly, the potential Eq. (2), which has a simple

Table 2. Calculated masses of heavy mesons and baryons. All results are in MeV.

Meson	Exp.	AL1	AP1	AL2	AP2
η_c	2983	2986	2975	2978	2983
J/ψ	3096	3095	3100	3091	3096
$\bar{D}$	1869	1862	1876	1860	1868
$\bar{D}^*$	2007	2014	2015	2019	2000
Baryon					
N	938	943	932	936	946
Λ_c	2286	2285	2290	2283	2279
Σ_c	2455	2471	2463	2475	2482
Σ_c^*	2520	2525	2541	2534	2533

form, i.e., it has no many-body forces and tensor forces, reproduced masses of the observed states quite well. Motivated by these results, we obtained mass values of the newly observed pentaquark states according to their quantum numbers. Table 3 shows the results of $J^P = 1/2^-$ case and Table 4 shows $J^P = 3/2^-$ case, respectively.

It can bee seen from Tables 3 and 4 show that the mass of $P_c(4312)$ of four potentials with the quantum number assignment $J^P = 1/2^-$ is more favourable than the quantum number $J^P = 3/2^-$. In contrast, the mass of $P_c(4440)$ and $P_c(4457)$ with the quantum number assignment $J^P = 3/2^-$ is more favourable than the the quantum number assignment $J^P = 1/2^-$. All the potentials reproduced the experimental data rather well.

In addition to the observed states, there are three six states with $J^P = 1/2^-$ and $J^P = 3/2^-$. We also calculated their mass values, which are shown in Table 5 for $J^P = 1/2^-$ and in Table 6 $J^P = 3/2^-$. These states are denoted as P_i, where $i = 1, \cdots 6$.

Two of these states lie below the $J/\psi p$ threshold, one of them is above the threshold for $J^P = 1/2^-$, and three of them are slightly above the $J/\psi p$ threshold for $J^P = 3/2^-$.

Table 3. Calculated masses of pentaquark states for $J^P = 1/2^-$. All results are in MeV.

State	Mass	AL1	AP1	AL2	AP2
$P_c(4312)$	$4311.9 \pm 0.7^{+6.8}_{-0.6}$	4314	4317	4320	4312
$P_c(4440)$	$4440.3 \pm 1.3^{+4.1}_{-4.7}$	4360	4371	4372	4374
$P_c(4457)$	$4457.3 \pm 0.6^{+4.1}_{-1.7}$	4390	4388	4395	4392

Table 4. Calculated masses of pentaquark states for $J^P = 3/2^-$. All results are in MeV.

State	Mass	AL1	AP1	AL2	AP2
$P_c(4312)$	$4311.9 \pm 0.7^{+6.8}_{-0.6}$	4371	4382	4377	4369
$P_c(4440)$	$4440.3 \pm 1.3^{+4.1}_{-4.7}$	4441	4445	4439	4445
$P_c(4457)$	$4457.3 \pm 0.6^{+4.1}_{-1.7}$	4456	4458	4450	4457

Table 5.   Predicted masses of pentaquark states for $J^P = 1/2^-$. All results are in MeV.

State	AL1	AP1	AL2	AP2
P_1	3978	3964	4005	3994
P_2	4021	4015	4039	4028
P_3	4075	4059	4051	4062

Table 6.   Predicted masses of pentaquark states for $J^P = 3/2^-$. All results are in MeV.

State	AL1	AP1	AL2	AP2
P_4	4099	4102	4114	4089
P_5	4125	4120	4130	4118
P_6	4154	4162	4165	4177

This may require a different strategy for observing these states. A further detailed study of the $J/\psi p$ invariant mass spectrum can elucidate the status of these states.

The method of ANN for solving differential and eigenvalue equations includes a trial function [41]. A trial function can be written as a feed-forward neural network, which includes adjustable parameters (weights and biases). The eigenvalue is refined to the existing solutions by training the neural network. As mentioned in Ref. [26], if a wave function results in a multiquark configuration an energy as $E = 100$ MeV below the lowest threshold, it can represent the exact solution of the system. Moreover, an energy of $E = 100$ MeV above one of the threshold poses a question mark about the wave function and the model for describing the system. The relevant thresholds have been calculated in Ref. [25] as 4329 MeV for $D\Sigma_c$ with $I(J^P) = \frac{1}{2}(\frac{1}{2})^-$ and 4483 MeV for $D^*\Sigma_c$ with $I(J^P) = \frac{1}{2}(\frac{3}{2})^-$. Our mass values are below these values, at the order of 50 MeV of the relevant thresholds, which means that the trial function of this work represents the five-body structure quite well.

The LHCb result could be important to understand the heavy quark spin symmetry (HQSS). In the limit where the masses of heavy quarks are taken to infinity, the spin of the quark decouples from the dynamics, which refers that the strong interactions in the system are independent of the heavy quark spin. This implies that the states that differ only in the spin of the heavy quark, i.e., states in which the rest of the system has the same total angular momentum, should be degenerate. This is also the case for single heavy baryons like $\Sigma_c^* \Sigma_b^*$ and referred to as the heavy quark spin (HQS) multiplet structure. Refs. [38, 39] show that the HQS multiplet structure predicts a state near $\bar{D}^*\Sigma_c^*$ threshold with $J^P = 5/2^-$. The $\bar{D}^*\Sigma_c^*$ threshold with $J^P = 5/2^-$ was calculated in Ref. [25] as 4562 MeV. Our mass estimation for this state is shown in Table 7.

A $5/2^-$ $\bar{D}^*\Sigma_c^*$ state does not couple to the $J/\psi p$ in S-

Table 7.   Mass prediction of pentaquark state for $J^P = 5/2^-$. All results are in MeV.

	AL1	AP1	AL2	AP2
Mass	4478	4469	4460	4461

wave, therefore it is not expected to exhibit a peak in the LHCb [39]. In fact, the phase space rather than partial wave dependence determines whether a state can produce a peak or not. The $J/\psi p$ threshold is around 4040 MeV, which is far below the mass of the P_c state. Given a sufficiently large coupling, this can produce a peak in the $J/\psi p$ invariant mass spectrum even though the high partial wave is large. Hence, there is still enough room to observe this state.

4   Summary and concluding remarks

Inspired by the recent observation of the hidden-charm pentaquark states, we solved the five-body Schrödinger equation within the nonrelativistic quark model framework. We used a nonrelativistic quark model using the potentials proposed in [44]. These potentials reproduced the experimental ground state masses of some mesons and baryons as a demonstration of the method. We employed the ANN method to obtain the solution of the five-body Schrödinger equation.

We gave a prediction of quantum numbers for these newly observed pentaquarks. The quantum number assignments for $P_c(4312)$, $P_c(4440)$, and $P_c(4457)$ of this work are in agreement with [33, 34, 36, 38]. Since the spin and parity numbers are not determined in the LHCb report, the other J^P assignments cannot be excluded. For example, the $P_c(4440)$ and $P_c(4457)$ states can be described as $5/2^+$ and $5/2^-$ $\bar{D}^*\Sigma_c$ states, respectively [15]. Partial wave analysis in the experimental data is critical to elucidate the internal structures of these exotic states.

We also calculated the mass for the $5/2^-$ $\bar{D}^*\Sigma_c^*$ state, which is a prediction of heavy quark spin multiplet structure. The average mass value of four estimations is roughly 95 MeV below the relevant threshold. Searching this missing HQS partner or partners is an important task for future experiments.

Within the framework of Hamiltonian in this study, a molecular picture for the newly observed pentaquark states cannot be concluded or excluded. Both the mass uncertainties and decay properties should be studied. The kinematic vicinity of the observed pentaquark states to the charmed meson-charmed baryon thresholds does not corroborate that they are molecules. In Ref. [49], it is found that masses and decay properties of the $P_c(4457)^+$, $P_c(4440)^+$, and $P_c(4312)^+$ can be understood if one treats them as $J^P = 3/2^-$, $J^P = 1/2^-$ and $J^P = 3/2^-$, compact pentaquark states, respectively. These properties can also

be obtained in the molecule picture, assuming $J^P = 3/2^-$ $(1/2^-)$, $J^P = 1/2^-$ $(3/2^-)$, and $J^P = (1/2^-)$ S-wave states, respectively.

References

1 S.-K. Choi et al (Belle Collaboration), Phys. Rev. Lett., **91**: 262001 (2003), arXiv:hep-ex/0309032

2 V.M. Abazov et al, Phys. Rev. Lett., **117**: 022003 (2016), arXiv:1602.07588[hep-ex]

3 V.M. Abazov et al, Phys. Rev. D, **97**: 092004 (2018), arXiv:1712.10176[hep-ex]

4 R. Aaij et al, Phys. Rev. Lett., **115**: 072001 (2015), arXiv:1507.03414[hep-ex]

5 J. J. Wu, R. Molina, E. Oset et al, Phys. Rev. Lett., **105**: 232001 (2010), arXiv:1007.0573v1[nucl-th]

6 Z. C. Yang, Z. F. Sun, J. He et al, Chin. Phys. C, **36**: 6 (2012), arXiv:1105.2901[hep-ph]

7 W. L. Wang, F. Huang, Z. Y. Zhang et al, Phys. Rev. C, **84**: 015203 (2011), arXiv:1101.0453[nucl-th]

8 J. J. Wu, T.-S. H. Lee, and B. S. Zou, Phys. Rev. C, **85**: 044002 (2012), arXiv:1202.1036[nucl-th]

9 C. Garcia-Recio, J. Nieves, O. Romanets et al, Phys. Rev. D, **87**: 074034 (2013), arXiv:1302.6938[hep-ph]

10 R. Chen, X. Liu, X. Q. Li et al, Phys. Rev. Lett., **115**: 132002 (2015), arXiv:1507.03704[hep-ph]

11 M. Karliner and J. L. Rosner, Phys. Rev. Lett., **115**: 122001 (2015), arXiv:1506.06386[hep-ph]

12 L. Roca, J. Nieves, and E. Oset, Phys. Rev. D, **92**: 094003 (2015), arXiv:1507.04249[hep-ph]

13 U. G. Meißner and J. A. Oller, Phys. Lett. B, **751**: 59 (2015), arXiv:1507.07478[hep-ph]

14 H. X. Chen, W. Chen, X. Liu et al, Phys. Rev. Lett., **115**: 172001 (2015), arXiv:1507.03717[hep-ph]

15 J. He, Phys. Lett. B, **753**: 547 (2016), arXiv:1507.05200[hep-ph]

16 T. Uchino, W. H. Liang, and E. Oset, Eur. Phys. J. A, **52**: 43 (2016), arXiv:1504.05726[hep-ph]

17 Y. Shimizu, D. Suenaga, and M. Harada, Phys. Rev. D, **93**: 114003 (2016), arXiv:1603.02376[hep-ph]

18 Y. Yamaguchi and E. Santopinto, Phys. Rev. D, **96**: 014018 (2017), arXiv:1606.08330[hep-ph]

19 K. Azizi, Y. Sarac, and H. Sundu, Phys. Rev. D, **95**: 094016 (2017), arXiv:1612.07479[hep-ph]

20 L. Maiani, A. D. Polosa, and V. Riquer, Phys. Lett. B, **749**: 289 (2015), arXiv:1507.04980[hep-ph]

21 R. F. Lebed, Phys. Lett. B, **749**: 454 (2015), arXiv:1507.05867[hep-ph]

22 G. N. Li, X. G. He, and M. He, JHEP, **12**: 1-17 (2015), arXiv:1507.08252[hep-ph]

23 Z. G. Wang, Eur. Phys. J. C, **76**: 70 (2016), arXiv:1508.01468[hep-ph]

24 W. Park, A. Park, S. Cho et al, Phys. Rev. D, **95**: 054027 (2017), arXiv:1702.00381[hep-ph]

25 J.-M. Richard, A. Valcarce, and J. Vijande, Phys. Lett. B, **774**: 710-714 (2017), arXiv:1710.08239[hep-ph]

26 E. Hiyama, A. Hosaka, M. Oka et al, Phys. Rev. C, **98**: 045208 (2018), arXiv:1803.11369[nucl-th]

27 G. Yang and J. Ping, Phys. Rev. D, **95**: 014010 (2017), arXiv:1511.09053[hep-ph]

28 S. Takeuchi and M. Takizawa, Phys. Lett. B, **764**: 254 (2017), arXiv:1608.05475[hep-ph]

29 V. Kubarovsky and M. B. Voloshin, Phys. Rev. D, **92**: 031502 (2015), arXiv:1508.00888[hep-ph]

30 T. Skwarnicki on behalf of the LHCb collaboration, Hadron spectroscopy and exotic states at LHCb, talk given at Moriond 2019, moriond.in2p3.fr/QCD/2019/TuesdayMorning/ Skwarnicki. pptx, arXiv: 1904.03947[hep-ex]

31 Z.-H. Guo and J. A. Oller, arXiv: 1904.00851[hep-ph]

32 C.-J. Xiao, Y. Huang, Y.-B. Dong et al, arXiv: 1904.00872[hep-ph]

33 J. He, arXiv: 1903.11872[hep-ph]

34 H. X. Chen, W. Chen, and S. L. Zhu, arXiv: 1903.11001[hep-ph]

35 R. Chen, Z. F. Sun, X. Liu et al, arXiv: 1903.11013[hep-ph]

36 F. K. Guo, H. J. Jing, U. G. Meissner et al, arXiv: 1903.11503[hep-ph]

37 M. Z. Liu, Y. W. Pan, F. Z. Peng et al, arXiv: 1903.11560[hep-ph]

38 Y. Shimizu, Y. Yamaguchi, M. Harada et al, arXiv: 1904.00587[hep-ph]

39 C. W. Xiao, J. Nieves, E. Oset et al, arXiv: 1904.01296[hep-ph]

40 I.E. Lagaris, A. Likas, and D.I. Fotiadis, Comput. Phys. Commun., **104**: 1-14 (1997), arXiv:quant-ph/9705029

41 I.E. Lagaris, A. Likas, and D.I. Fotiadis, IEEE T. Neural Networ., **9**: 987-1000 (1998), arXiv:physics/9705023[physics.comp-ph]

42 D. R. Parisi, M. C. Mariani, and M. A.Laborde, Chem. Eng. Process., **42**: 715-721 (2003)

43 N. Yadav, A. Yadav, and M. Kumar, *An Introduction to Neural Network Methods for Differential Equations*, (Springer, 2015)

44 C. Semay and B. Silvestre-Brac, Z. Phys. C, **61**: 271-275 (1994)

45 S. Haykin, *Neural Networks: A Comprehensive Foundation, 2nd ed*, (Prentice-Hall: New York, USA, 1999)

46 M. Sugawara, Comput. Phys. Commun., **140**: 366-380 (2001)

47 J. M. Zurada, *Introduction to Artificial Neural Systems*, (West Publishing Co., St. Paul, MN, 1992)

48 A. Alex, M. Kalus, A. Huckleberry et al, J. Math. Phys., **52**: 023507 (2011), arXiv:1009.0437[math-ph]

49 J.-B. Cheng and Y.-R. Liu, arXiv: 1905.08605[hep-ph]